JOURNAL OF MATERIALS SCIENCE 23 (1988) 3671–3677

A statistical fracture mechanics analysis of time-dependent strength behaviour of partially stabilized zirconia

KAI DUAN, YIU-WING MAI, BRIAN COTTERELL
Department of Mechanical Engineering, University of Sydney, Sydney, New South Wales 2006, Australia

The time-dependent strength behaviour of a partially stabilized zirconia ceramic (Mg-PSZ) when subjected to constant static and cyclic stresses as well as constant stress rates is analysed in terms of a statistical fracture mechanics model given earlier by the authors. Given the lifetimes for either constant static stresses or constant stress rates it is possible to estimate the lifetimes for constant cyclic stresses. There is good agreement between the predicted and actual lifetimes under cyclic stresses if the data for constant stress rates are used with the theory. The limitations of the conventional single-crack theory for lifetime predictions relative to the statistical fracture mechanics approach are highlighted.

1. Introduction

There are two main factors which control the lifetimes of structural components made from ceramic materials. One is geometrical, being characterized by the statistical distribution of flaw sizes due to the compacting and sintering process as well as any subsequent shaping operations; the other is mechanical, due to the spreading of the pre-existing flaws enhanced by a stress-corrosion mechanism at the flaw tips [1–3]. Accurate lifetime predictions can only be made if these two factors are properly considered in the evaluation procedures. Conventionally, the geometrical factor is discarded in the lifetime analysis since it is thought that the largest single flaw determines the strength. The time-to-failure is then simply the time required for that flaw to grow from an inherent size (a_i) to a critical size (a_c) at which time the fracture toughness (K_{Ic}) of the ceramic material is reached. The rate of crack growth (da/dt) is best described by the following power law relationship [3]:

$$da/dt = AK_a^n \quad (1)$$

where A is a material–environment constant, n is the stress-corrosion exponent and K_a is the applied stress intensity factor at the flaw tip. In previous papers [4, 5] the authors have developed a statistical time-dependent fracture model for brittle materials by including both the geometrical and mechanical factors. It is shown there that the single-crack approach always underestimates the failure lifetimes compared to the statistical fracture theory for cases where the samples are under constant sustained stresses (σ_a) and constant stress rates ($\dot{\sigma}_a$). For many ceramic materials with the Weibull modulus for inert strength distribution (m) between 5 and 20, and the stress-corrosion exponent (n) between 10 and 80, the difference is at most about 80%. This magnitude of difference is unfortunately difficult to discern from the experimental data because of the expected large scatter for brittle materials. However, for samples subjected to constant-amplitude cyclic stresses (σ_c) due to rotation bending in Wöhler machines, the predicted lifetimes to failure are much less for the statistical fracture model than the single-crack theory [5]. This has provided a simple discriminating test for the accuracy and usefulness of the two different approaches.

Swain [6] has recently obtained lifetime data for a magnesia-stabilized zirconia (Mg-PSZ, maximum strength (MS) grade from Nilcra, Melbourne, Australia) when subjected to constant static stresses, constant stress rates and cyclic stresses. He has shown that the single-crack theory is inconsistent with the cyclic stress data. In this paper the authors attempt to re-analyse these lifetime data using the statistical fracture model given earlier [4, 5].

2. Background theory

The details of the statistical fracture model for the time-dependence of strength of ceramic materials have already been given [4, 5]. In the following only the basic equations which are required to analyse the lifetime data in Section 3 are presented.

By assuming the flaws to be randomly distributed within the volume V of the sample and the flaw size distribution $q(a)$ to follow a Pareto function,

$$q(a) = \left(\frac{\varrho_f m}{2a_0}\right)\left(\frac{a_0}{a}\right)^{(m+2)/2} \qquad a_0 \leqslant a$$
$$q(a) = 0 \qquad a < a_0 \quad (2)$$

where ϱ_f is the flaw density and a_0 is the smallest flaw, it can be shown that the failure probability at stress σ_a [7] is

$$F(\sigma_a) = 1 - \exp\left[-\int_V \int_{a(\sigma_a)}^{\infty} q(a)\,da\,dV\right] \quad (3)$$

0022–2461/88 $03.00 + .12

It is also assumed that ϱ_f is small so that there is no flaw interaction and a is the equivalent length of the Griffith flaw lying normal to the maximum principal stress.

In the statistical fracture model it is realised that all the flaws will spread with time t under a given applied stress σ_a, and the growth rate of each individual flaw is determined by Equation 1. This means that the flaw size distribution $q(a)$ will change with time to $q(a, t)$. If there are no new flaws nucleated during this stage it can be shown [5] that

$$\int_{a(\sigma_a)}^{\infty} q(a, t)\,da = \int_{a_r(\sigma_a,t)}^{\infty} q(a)\,da \quad (4)$$

where a_r is the reference flaw size at $t = 0$ and is related to size a at time t [5] by

$$a_r(\sigma_a, t) = \left[1 + \left(\frac{n}{2} - 1\right) AY^2K_{Ic}^{n-2}\sigma_a^2 t\right]^{2/(2-n)} a(\sigma_a) \quad (5)$$

where Y is a geometry correction factor.

The failure probabilities can now be derived from Equation 3 by replacing $q(a)$ with $q(a, t)$ and using Equations 4 and 5 when performing the integration, i.e.

$$F(\sigma_a, t_f) = 1 - \exp\left[-\int_V \int_{a_r(\sigma,t_f)}^{\infty} q(a)\,da\,dV\right] \quad (3a)$$

The stresses acting at the flaws (σ) are a function of σ_a and depend on their positions (x, y) within the volume of the sample.

In Swain's experiments, the lifetime data for constant sustained stresses (σ_a) and constant stress rates ($\sigma_a = \dot{\sigma}_a t$) were obtained from rectangular cross-section samples under four- and three-point bending, respectively; but the lifetime data for constant-amplitude cyclic stresses (σ_c) in rotation bending were derived from circular cross-section rods. Noting these differences in specimen geometry and loading configuration in the integration of Equation 3a, the following lifetime prediction equations are obtained [5]. Thus

$$t_f\sigma_a^n = \bar{\lambda}_{s4} = \frac{2\sigma_{*4}^{n-2}}{(n-2)AY^2K_{Ic}^{n-2}} \times \left[\left(\frac{mn + n - 2}{(m+1)(n-2)}\right) \ln\left(\frac{1}{1-F}\right)\right]^{(n-2)/m} \quad (6)$$

for the constant sustained stress case (i.e. σ_a = constant),

$$\sigma_f^{n+1} = (t_f\dot{\sigma}_a)^{n+1} = \dot{\sigma}_a\bar{\lambda}_{d3} = \frac{2\dot{\sigma}_a\sigma_{*3}^{n-2}(n+1)}{(n-2)AY^2K_{Ic}^{n-2}} \times \left[\left(\frac{mn + n - 2}{(m+1)(n-2)}\right)^2 \ln\left(\frac{1}{1-F}\right)\right]^{(n-2)/m} \quad (7)$$

for the constant stress rate case (i.e. $\dot{\sigma}_a$ = constant), and finally

$$t_f\sigma_c^n = \bar{\lambda}_c = \frac{2\sigma_{*c}^{n-2}\pi}{(n-2)AY^2K_{Ic}^{n-2}} \times \left[\left(\frac{mn + 2n - 4}{2(n-2)}\right) \times \ln\left(\frac{1}{1-F}\right)\right]^{(n-2)/m} \Big/ \int_0^{\pi/2} \sin^n x\,dx \quad (8)$$

for the rotation bending case in which $\sigma_a = \sigma_c \sin \omega t$ and ω is the frequency. In Equations 6 to 8 the normalized stress parameters σ_* are given by

$$\sigma_{*4} = \sigma_0\left(\frac{2(m+1)}{V_4\varrho_f}\right)^{1/m}$$
$$\sigma_{*3} = \sigma_0\left(\frac{2(m+1)^2}{V_3\varrho_f}\right)^{1/m} \quad (9)$$
$$\sigma_{*c} = \frac{\sigma_0}{(V_c\varrho_f)^{1/m}}$$

where the subscripts 3, 4 and c for V indicate the mode of loading and σ_0 is related to the smallest flaw size a_0 by

$$\sigma_0 = K_{Ic}Y(a_0)^{1/2} \quad (10)$$

and $Y = (2/\pi)^{1/2}$ for a penny-shaped crack. In deriving Equation 8 it is assumed that the cyclic fatigue effect is negligible.

Now, given the lifetime data for either constant sustained stress or constant stress rate it is possible to predict lifetimes of the other as well as those for constant-amplitude cyclic stress from Equations 6 to 8. This is because the constants $\bar{\lambda}_{s4}$, $\bar{\lambda}_{d3}$ and $\bar{\lambda}_c$ are interconnected by

$$\frac{\bar{\lambda}_{s4}}{\bar{\lambda}_{d3}} = \left(\frac{1}{n+1}\right)\left(\frac{V_3(n-2)}{V_4(mn + n - 2)}\right)^{(n-2)/m} \quad (11a)$$

$$\frac{\bar{\lambda}_{s4}}{\bar{\lambda}_c} = \frac{1}{\pi}\left(\frac{4(mn + n - 2)V_c}{(mn + 2n - 4)V_4}\right)^{(n-2)/m} \int_0^{\pi/2} \sin^n x\,dx \quad (11b)$$

$$\frac{\bar{\lambda}_{d3}}{\bar{\lambda}_c} = \left(\frac{n+1}{\pi}\right)\left(\frac{4(mn + n - 2)^2V_c}{(n-2)(mn + 2n - 4)V_3}\right)^{(n-2)/m} \times \int_0^{\pi/2} \sin^n x\,dx \quad (11c)$$

In the single-crack approach for lifetime predictions it is possible to combine the Weibull inert strength distribution function [8]

$$F(\sigma_a) = 1 - \exp\left[-(\sigma_a/\sigma_*)^m\right] \quad (12)$$

in the calculations. This technique has been used by Jakus *et al.* [9] and the lifetime equations [5] are

$$t_f\sigma_a^n = \lambda_s = \frac{2\sigma_*^{n-2}}{(n-2)AY^2K_{Ic}^{n-2}}\left[\ln\left(\frac{1}{1-F}\right)\right]^{(n-2)/m} \quad (13)$$

$$(t_f\dot{\sigma}_a)^{n+1} = \sigma_f^{n+1} = \dot{\sigma}_a\lambda_d = \frac{2\dot{\sigma}_a(n+1)\sigma_*^{n-2}}{(n-2)AY^2K_{Ic}^{n-2}} \times \left[\ln\left(\frac{1}{1-F}\right)\right]^{(n-2)/m} \quad (14)$$

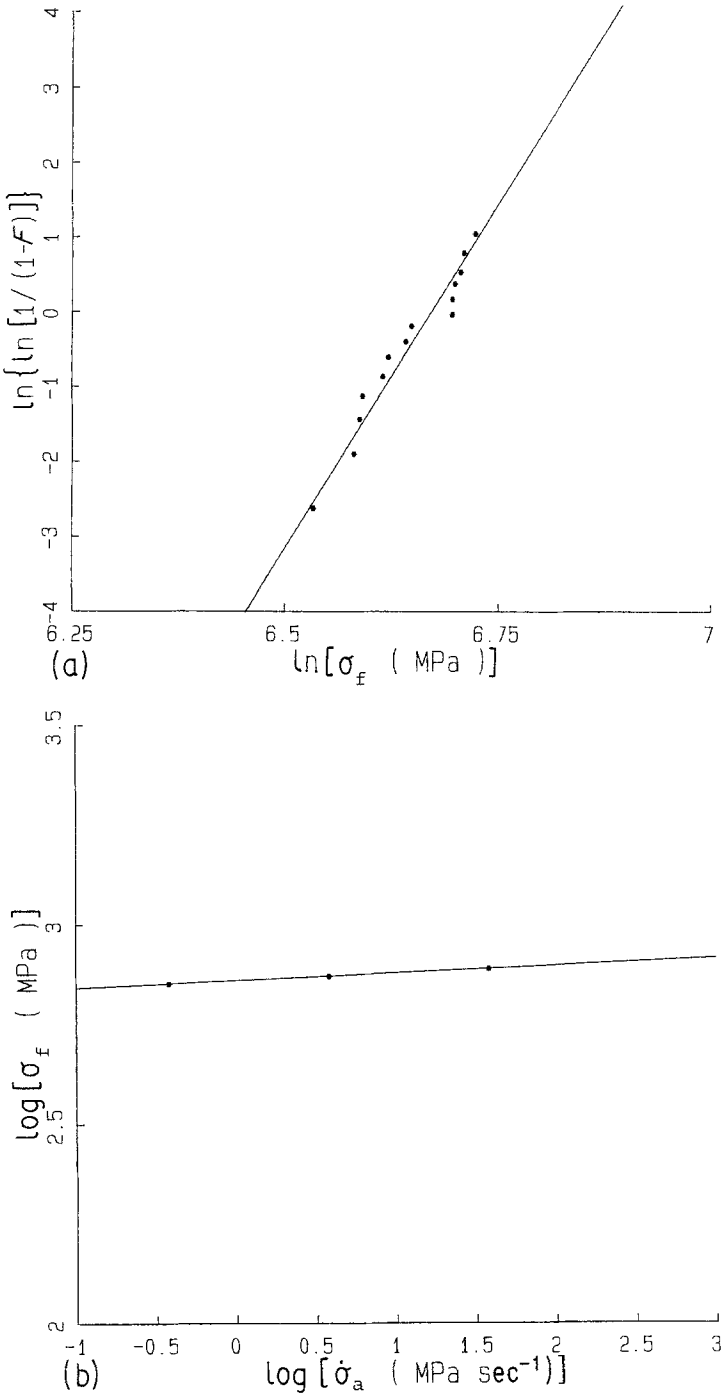

Figure 1 (a) Strength distribution of MS-grade Mg-PSZ ceramic at a constant stress rate of 38 MPa sec^{-1} at room temperature (m = 17.4). (b) Bend strength (three-point loading) as a function of stress rate. (After Swain [6]).

and

$$t_f\sigma_c^n = \lambda_c = \frac{2\sigma_*^{n-2}\pi}{(n-2)AY^2K_{Ic}^{n-2}} \times \left[\ln\left(\frac{1}{1-F}\right)\right]^{(n-2)/m} \Big/ \int_0^{\pi/2} \sin^n x\,dx \quad (15)$$

for the constant sustained stress, constant stress rate and cyclic stress cases, respectively. Note that these equations do not depend on the specimen geometry and loading configuration. The relations between the constants λ_s, λ_d and λ_c are given by

$$\frac{\lambda_s}{\lambda_d} = \frac{1}{n+1} \quad (16a)$$

$$\frac{\lambda_s}{\lambda_c} = \frac{1}{\pi}\int_0^{\pi/2} \sin^n x\,dx \quad (16b)$$

$$\frac{\lambda_d}{\lambda_c} = \left(\frac{n+1}{\pi}\right)\int_0^{\pi/2} \sin^n x\,dx \quad (16c)$$

Interestingly, unlike the statistical fracture approach, the Weibull modulus m does not enter into any of Equations 16. The ratios of the λ constants are only determined by the stress-corrosion exponent n.

3. Comparison of theory with experimental data

Figs 1–3 show the experimental data obtained by Swain [6] on an Mg-PSZ ceramic for the three cases of constant stress rates, constant sustained and cyclic stresses, respectively. Using Equation 7 and Fig. 1b the stress-corrosion exponent n is determined to be 52.8 and $\log_{10}\bar{\lambda}_{d3}$ is 153.86 for a 50% failure probability. Fig. 1a shows the Weibull plot of the fracture strength at a stress rate of 38 MPa sec^{-1} and this gives an effective Weibull modulus m^* of 17.4. In Hu *et al.* [5] it is shown that the true Weibull modulus (m) defined in Equation 2 is increased to m^* by slow

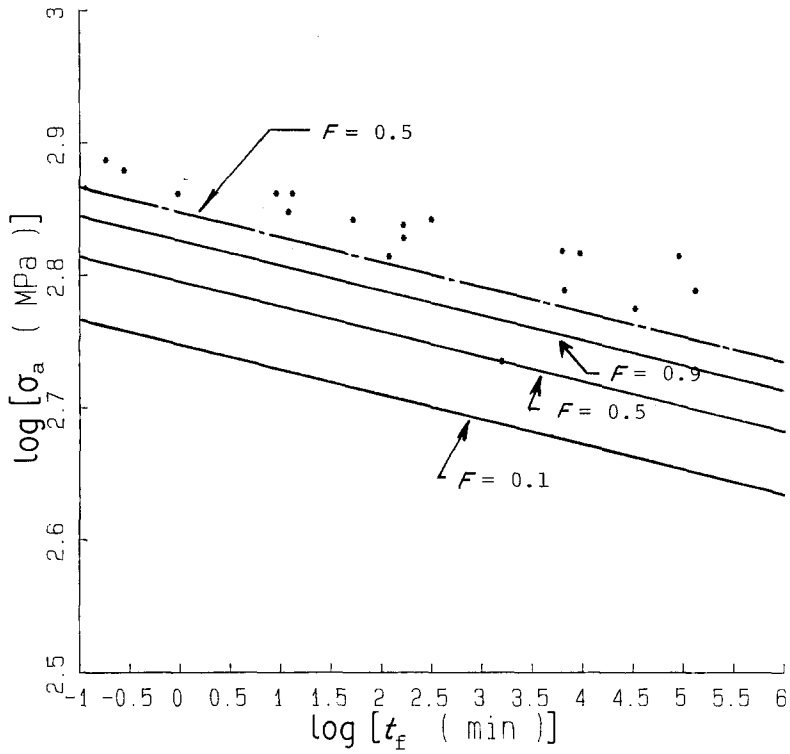

Figure 2 (∗) Lifetime data for Nilcra's MS-grade Mg-PSZ tested in static four-point loading. (After Swain [6]). (——) Predicted from statistical model using constant stress rate data in Fig. 1; (–·–·–) predicted using single-crack theory.

crack growth [9–11] and

$$m = m^*(n - 2)/(n + 1) \quad (17)$$

so that $m = 16.4$. Now Equation 11a can be used to obtain $\bar{\lambda}_{s4}$ since m, n, V_3, V_4 and $\bar{\lambda}_{d3}$ are all given and lifetime predictions for the static lifetime data can be made from Equation 6 for given failure probabilities. These predictions are given in Fig. 2 but they all fall below the experimental data.

To use the constant stress rate data to predict lifetimes under cyclic stress in rotation bending, $\bar{\lambda}_c$ can be obtained using Equation 11c which in turn can be used in Equation 8. These lifetime prediction lines for $F = 0.1$, 0.5 and 0.9 are shown in Fig. 3 and they appear to agree well with the experimental results.

The cyclic lifetime data can also be predicted from the constant stress lifetime results shown in Fig. 2. A least-squares fit to these data shows that $n = 56$ and $\log_{10}\bar{\lambda}_{s4} = 160.91$. $\bar{\lambda}_c$ can then be calculated from Equation 11b and used in Equation 8 for lifetime predictions. However, as shown in Fig. 3, these predictions overestimate the real cyclic data.

Using the dynamic strength data from Fig. 1 and the single-crack theory, λ_d and n can be determined using Equation 14. λ_s and λ_c are calculated from Equation 16 and used in conjunction with Equations 14 and 15 for lifetime predictions under static and cyclic stresses. These predictions are also shown in Figs 2 and 3 for 50% failure probability. Similarly, the static lifetime data of Fig. 2 can be used to predict the

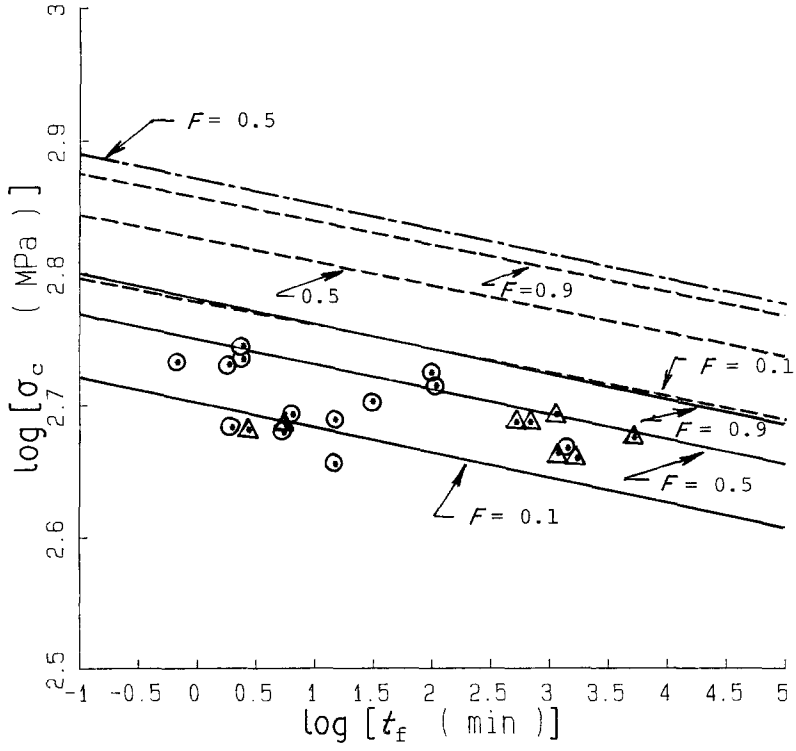

Figure 3 Cyclic lifetime data for Nilcra's MS-grade Mg-PSZ for (⊙) 200 Hz and (△) 15.5 Hz. (After Swain [6]). (——) Predicted from statistical model using constant stress rate data in Fig. 1; (– – –) predicted from statistical model with static data in Fig. 2; (–·–·–) predicted from single-crack theory.

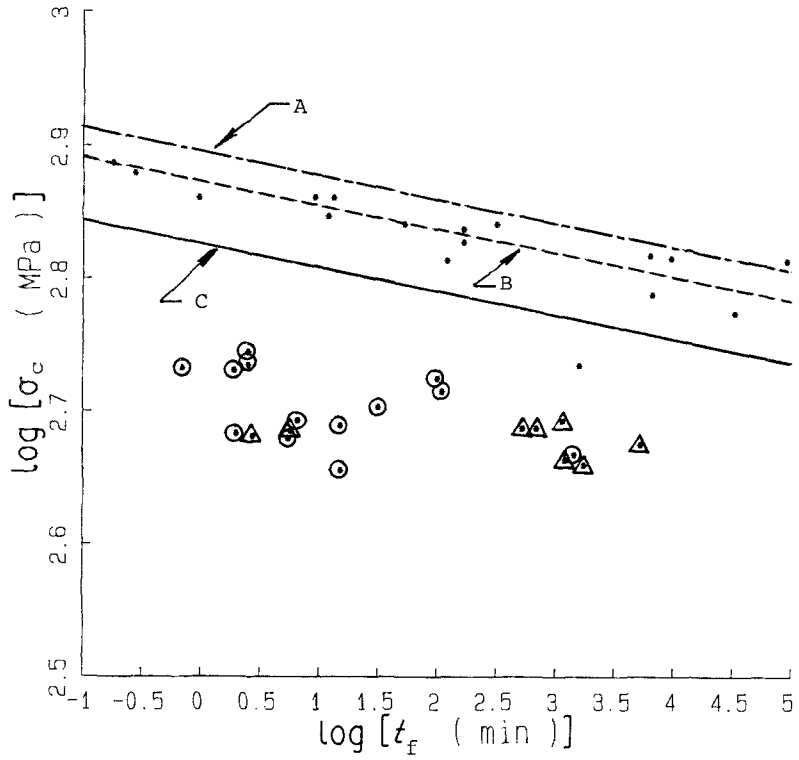

Figure 4 Comparison of cyclic lifetime data with predicted lines: (A) from single-crack theory and (C) from statistical model using the static data represented by (B) the line of best fit. Note that the correct trend is predicted by the statistical crack approach. All prediction lines are for $F = 0.5$. (⊙, △) As in Fig. 3.

lifetimes under cyclic stresses using the single-crack theory. Fig. 4 shows that the predicted values for $F = 0.5$ are larger than the static lifetime data, whereas the statistical fracture approach shows these to be less.

4. Discussion

A comparison of the lifetime experimental results given in Figs 2 and 3 shows that the lifetimes under cyclic stresses are much less than those obtained for static stresses of the same magnitude. This has led Swain [6] to postulate that cyclic fatigue, much as in polymers and metals, may exist due to the non-linear stress–strain behaviour of the Mg-PSZ ceramics. However, the non-linear plasticity is very limited in the MS grade of this Nilcra material and is not as extensive as in the TS grade. In addition, the lifetimes for cyclic loading is approximately independent of frequency (15.5 and 200 Hz), suggesting that any cyclic fatigue effects would be small. On the contrary, frequency usually has a pronounced effect on stress-corrosion fatigue in metals and polymers [3].

Swain [6] noted that the cyclic lifetime data are inconsistent with the single-crack theory since it can be easily shown from Equation 16b that

$$t_{fc} = t_{fs}\left(\frac{\sigma_a}{\sigma_c}\right)^n \left(\frac{\lambda_c}{\lambda_s}\right)$$

$$= t_{fs}\left(\frac{\sigma_a}{\sigma_c}\right)^n \pi \Big/ \int_0^{\pi/2} \sin^n x \, dx \qquad (18)$$

where the second subscript of t indicates "cyclic" and "static" stresses, respectively. For $\sigma_a = \sigma_c$, $t_{fc} > t_{fs}$ since $\lambda_c/\lambda_s > 1.0$. This prediction is, therefore, opposite to the actual cyclic lifetime data. With the statistical fracture theory Equation 11b gives

$$t_{fc} = t_{fs}\left(\frac{\sigma_a}{\sigma_c}\right)^n \left(\frac{\bar{\lambda}_c}{\bar{\lambda}_{s4}}\right)$$

$$= t_{fs}\left(\frac{\sigma_a}{\sigma_c}\right)^n \pi \left(\frac{(mn + 2n - 4)V_4}{4(mn + n - 2)V_c}\right)^{(n-2)/m} \Big/ \int_0^{\pi/2} \sin^n x \, dx \qquad (19)$$

Again for $\sigma_a = \sigma_c$, $\bar{\lambda}_c/\bar{\lambda}_{s4} < 1.0$ for $m = 16.4$ and $n = 52.8$ so that $t_{fc} < t_{fs}$ as confirmed by the static and cyclic data shown in Fig. 4. Unfortunately, the predicted lifetimes from the static data (i.e. Line C), are much larger than the experimental results and it is hence tempting to suggest that a cyclic fatigue does exist. This argument is fallacious since, from the statistical fracture theory, values of t_{fc} predicted from the constant stress rate results agree well with the experimental data given in Fig. 3. The fact that the static data fail to accurately predict the cyclic lifetime results can be explained as follows.

In the statistical fracture model developed in Section 2 it is assumed that all the samples for the three different kinds of test have the same flaw size distribution $q(a)$ within the volume of the material, being described by Equation 2. This means that ϱ_f, a_0 and m are the same and this can be achieved only if all the samples are manufactured in the same way. If so, it can be shown that

$$\frac{\sigma_{*4}}{\sigma_{*3}} = \left(\frac{V_3}{V_4(m + 1)}\right)^{1/m} \qquad (20)$$

from Equations 9 and 11a. Also, using the Weibull inert strength equation and for the same failure probability,

$$\frac{\sigma_{*4}}{\sigma_{*3}} = \frac{\sigma_{f4}}{\sigma_{f3}} \qquad (21)$$

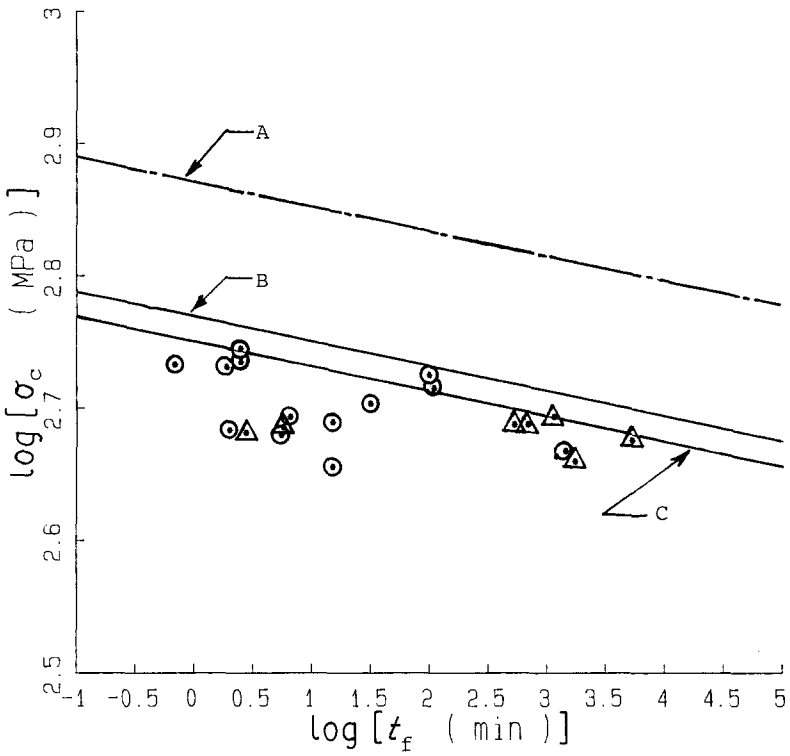

Figure 5 Comparison of cyclic lifetime data with predicted lines assuming (C) volume flaws or (B) surface flaws. Single-crack theory prediction (A) is independent of surface or volume flaws. All prediction lines are for $F = 0.5$. (⊙, △) As in Fig. 3.

where σ_f is the fracture strength. In Swain's experiments, $V_3 = 4\,\text{mm} \times 3\,\text{mm} \times 35\,\text{mm}$, $V_4 = 4\,\text{mm} \times 3\,\text{mm} \times 15\,\text{mm}$ and $m = 16.4$ so that $(\sigma_{*4}/\sigma_{*3}) = 0.89$ from Equation 20. However, inert strength measurements are not available, but σ_{f4}/σ_{f3} can be estimated to a first approximation from Figs 1b and 2 when the time to failure is small (here in this case $t_f = 6$ sec) and this gives $\sigma_{f4}/\sigma_{f3} = 0.99$, which is larger than the theoretical value. Although this difference appears to be small (i.e. 0.89 compared with 0.99), if it is corrected for in the calculations, the net effect is to move up all the lifetime prediction lines for the constant stress rate data to the positions occupied by the corresponding lines of the single-crack theory shown in Fig. 2.

It is realised that all the samples used for the three different kinds of experiment were machined and ground. Hence, the time-dependent strength properties are more likely to be determined by surface flaws generated by the shaping process. The theory developed in Section 2 can be modified to account for surface rather than volume flaws [5] provided that Equations 1 and 2 are still valid. Without going into mathematical details, it suffices to say from Fig. 5 that there is little difference in lifetime predictions, whether surface or volume flaws are to be used in the theory. Once again, the inert strength results for three- and four-point bending do not agree with the theoretical Weibull prediction. These observations leave the authors with only one plausible conclusion, namely that the flaw size distribution function of the constant sustained stress (four-point bending) samples is different to that of the constant stress rate (three-point bending) and cyclic stress samples.

Following Fuller *et al.* [12], Swain suggested that because of surface residual stresses due to machining and grinding the stress-corrosion exponent n obtained indirectly from the slopes of the static, dynamic and cyclic tests is less than that determined directly from large crack systems as in double cantilever beams (DCBs), i.e. 52.8 from Fig. 1b as opposed to 120 in DCB samples. This is unlikely to be the real cause, since in Swain's experiments on both annealed and polished samples (where the purpose is to remove the residual stresses associated with the shaping process), $n = 53$ and 54 in good agreement with $n = 52.8$ obtained from the constant stress rate results. However, it must not be concluded that surface residual stresses do not affect n – indeed they do, since Swain [6] has shown that in constant stress rate tests on Vickers pyramid (500 N) indented samples n drops to 33.

A more likely explanation for the disagreement of n between direct and indirect measurements is also given by Swain, who suggested the reason of a rising crack growth resistance (R) curve with crack extension. It is possible that the R-curve is dependent on specimen geometry, i.e. small-crack as against large-crack systems, and this will have the effect of reducing the crack tip stress intensity factor so that the slow crack growth Equation 1 is altered and n changed. The authors are currently developing a theoretical model encompassing both the R-curve and the slow crack growth law in lifetime predictions.

It is recognised that the theory presented in this paper assumes the Mg-PSZ material to be "pseudo" linear-elastic even though there is some limited plasticity prior to fracture. As the predicted lifetimes show (Fig. 3), this assumption is probably justified and little error is introduced. However, for other much tougher zirconia-based ceramics, the statistical fracture model given in Section 2 has to be modified to include other effects associated with the more prominent plasticity and transformation toughening process. For example,

the enhanced plasticity will generate genuine cyclic-fatigue-induced damage and this shortens the lifetime. Fatigue crack propagation rates in terms of the Paris power law equation [3] have to be obtained experimentally. Crack growth now depends on both Equation 1 and the Paris fatigue equation and their possible interactions. It should also be noted that because of plasticity the neutral axis will be shifted and this modifies the stresses acting on the flaws. In addition, associated with the transformation process, a new population of flaws may be generated and this is difficult to that of the pre-existing flaws. The spreading of cracks in a sample containing two flaw size distribution functions needs to be studied in more detail.

5. Conclusion

The main conclusion reached in this work is that the lifetime predictions for an Mg-PSZ ceramic in rotation bending can be determined from the constant stress rate data using the statistical fracture model. As opposed to the single-crack theory which predicts otherwise, the statistical flaw approach correctly predicts the cyclic lifetime values to be much less than those under constant sustained stresses of the same magnitude. There is little cyclic effect in this ceramic material. The failure of the constant-stress lifetime data to accurately predict the cyclic results is probably due to the different flaw size distribution functions for the two types of sample used in these experiments. Further improvements of the model are necessary to include other effects of pronounced plasticity, the crack growth resistance curve and the generation of new flaws associated with transformation toughening.

Acknowledgements

The authors wish to thank the CSIRO/Sydney University Collaborative Research Fund for the support of this work. The frequent assistance in the form of original data, discussion and comments received from M. V. Swain and X-Z. Hu is appreciated.

Note added in proof

Since the acceptance of this paper it has come to our attention that Dauskart *et al.* [13] have shown that in Mg–PSZ ceramics cyclic fatigue crack growth obeying the Paris power law equation can occur in compact specimens containing *large* cracks. How relevant these fatigue data are to the experiments conducted by Swain [6] on specimens containing only *small* cracks which are randomly distributed within the sample volume/surfaces is not obvious to us. This paper brings out the significance of the statistical fracture model to explain why the lifetime data in cyclic loadings cannot be predicted from the single crack theory and why they are much less than the lifetime data for static loadings. Perhaps, in view of Dauskart *et al.*'s latest finding, we should also investigate the additional effect of cyclic fatigue on lifetime predictions using small cracks.

References

1. S. M. WIEDERHORN, *J. Amer. Ceram. Soc.* **50** (1967) 407.
2. B. R . LAWN, "Fracture of Brittle Solids" (Cambridge University Press, Cambridge, 1975) Ch. 8.
3. A. G. ATKINS and Y-W. MAI, "Elastic and Plastic Fracture: Metals, Polymers, Ceramics, Composites, Biological Materials", (Ellis Horwood/John Wiley, Chichester, 1985) pp. 485 and 622.
4. X-Z. HU, Y-W. MAI and B. COTTERELL, *J. Mater. Sci. Lett.* **6** (1987) 462.
5. *Idem, Phil. Mag.* (1988) in press.
6. M. V. SWAIN, *Mater. Forum* **9** (1986) 34.
7. X-Z. HU, B. COTTERELL and Y-W. MAI, *Proc. R. Soc.* **A401** (1985) 251.
8. W. WEIBULL, *J. Appl. Mech.* **18** (1951) 293.
9. K. JAKUS, D. C. COYNE and J. E. RITTER, *J. Mater. Sci.* **13** (1978) 2071.
10. R. F. BULLOCK and H. H. CHENEY, *Res. Mechanica* **19** (1986) 35.
11. J. D. HELFINSTINE, *J. Amer. Ceram. Soc.* **60** (1980) 113.
12. E. R. FULLER, B. R. LAWN and R. F. COOK, *J. Amer. Ceram. Soc.* **66** (1983) 314.
13. DAUSKART *et al.*, *J. Amer. Ceram. Soc.* **70** (1987) C248.

Received 1 May
and accepted 20 July 1987